Study on the Kinetics of Surface Migration of Surface Modifying Macromolecules in Membrane Preparation

Daniel Eumine Suk, Geeta Chowdhury, and Takeshi Matsuura*

Industrial Membrane Research Institute, Department of Chemical Engineering, University of Ottawa, Ottawa, Ontario, Canada K1N 6N5

Roberto Martin Narbaitz

Department of Civil Engineering, University of Ottawa, Ottawa, Ontario, Canada K1N 6N5

Paul Santerre

Department of Biomaterials, Faculty of Dentistry, University of Toronto, Toronto, Ontario, Canada M5S 1G6

Gerald Pleizier and Yves Deslandes

ICPET, National Research Council Canada, Ottawa, Ontario, Canada

Received July 10, 2001; Revised Manuscript Received December 11, 2001

ABSTRACT: Surface modifying macromolecules (SMM) were synthesized and blended into the casting solution of poly(ether sulfone). The solution was cast to films with thickness of 0.12 and 0.24 mm. The cast films were placed in an oven with forced air circulation for periods of 3, 5, 7, and 2000 min to remove the solvent, before being immersed into water at 4 °C for gelation. The membranes so prepared were further dried and subjected to contact angle measurement and XPS (X-ray photoelectron spectroscopy) analysis. It was found that the contact angle increased as the solvent evaporation period increased. The increase in contact angle was faster when the membrane was thinner. According to the XPS analysis, after an initial time lag the surface fluorine content increased as the evaporation time increased and finally leveled off. The increase in surface fluorine content was also faster when the membrane was thinner. A kinetic model was established for the SMM surface migration.

Introduction

Membrane Surface Modifications. The membrane surface plays an important role in the membrane performance, as manifested by the structure of composite membranes that generally comprise two distinct layers made of two different polymeric materials, i.e., a thin surface layer that governs the selectivity and flux of composite membranes and a thick substrate layer that is porous and provides the mechanical strength.[1,2] The advantage of a composite membrane is that both the surface layer and the substrate can be chosen separately to provide the best membrane performance.[3]

The methods of surface modification in preparation of composite membranes can be classified into three groups: i.e., physical, chemical, and bulk modification.[4] Many of the surface modification methods are complicated and require at least an additional step in the membrane preparation process.

Surface Modification by Surface Modifying Macromolecules. Recognizing the drawbacks of conventional surface modification methods, an alternative approach was proposed for membrane surface modification.[5]

In a polymer blend, thermodynamic incompatibility between polymers usually causes demixing of polymers to occur. If the polymer system is equilibrated in air, the polymer with the lowest surface energy (hydrophobic polymer) will concentrate at the air interface and reduce the system's interfacial tension as a consequence. The preferential adsorption of a polymer of lower surface tension at the surface was confirmed by a number of researchers for a miscible blend of polystyrene/poly(vinyl ether),[6,7] for diblock and triblock copolymer of polystyrene/poly(ethylene oxide),[8,9] and for the blend of poly(methyl methacrylate)/poly(vinyl chloride).[10]

Based on the above concept, surface modifying macromolecules (SMMs) were synthesized and blended into polymer solutions. During the process of casting the polymer solution into a film and the removal of solvent by evaporation, SMMs migrate to the membrane surface, rendering the surface of the membrane ultimately obtained more hydrophobic than the bulk membrane phase (see Figure 1).

A type of surface modifying macromolecules specifically designed for this purpose has a copolymeric nature. It has an amphipathic structure consisting of a main polyurethane chain terminated with two low-polarity polymer chains. Since the surface characteristics are largely determined by the low-polarity components, they can be chosen to give a specific property. It is preferable to use a fluorine-based component due to additional features such as surface lubrication, reduced fouling, and increased chemical resistivity associated with the carbon−fluorine (C−F) bond. Figure 2 shows the molecular structure of a typical SMM. The solubility in the base polymer can depend on the additive's average molecular weight, its molecular structure, and its low-polarity component, which can be controlled by varying factors such as the main chain length, the number of C−F bond, and the type of chemicals used to synthesize the main chain.[5]

When SMMs were blended into a poly(ether sulfone) (PES) membrane, the contact angle of the surface

10.1021/ma011205a CCC: $22.00
Published on Web 03/09/2002

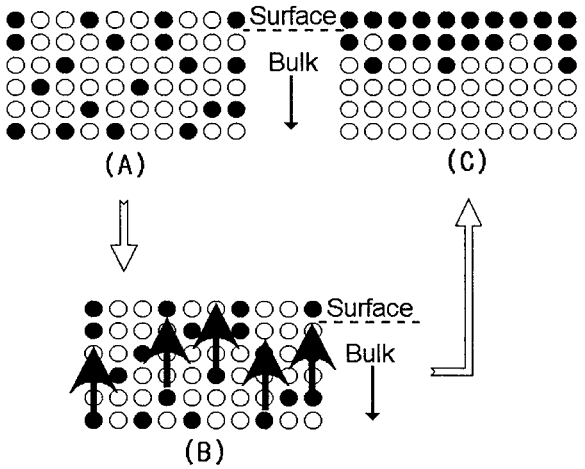

Figure 1. Schematic diagram illustrating SMM migration: ●, SMM molecule which has lower surface free energy; ○, base polymer. Case A: time zero; case B: time in between; case C: time infinite (taken from Ph.D. thesis of Y. Fang, 1996).

increased from 76° of PES to 116°, a value nearly equal to that of Teflon.[5] XPS analysis also confirmed that SMMs were concentrated at the surface of the membrane. These SMM blended PES membranes were found to remove chloroform effectively from water by pervaporation.[5] They were found to be less fouled in the treatment of cutting machine oil/water emulsion by ultrafiltration.[11] It was also found that the mechanical strength of PES membranes is generally enhanced by blending SMM into PES.[12]

SMM blended membranes were further characterized by XPS (X-ray photoelectric spectroscopy), SEM (scanning electron microscopy), and AFM (atomic force microscopy) to verify SMM migration and/or to find out effects of different membrane casting condition to SMM migration.[13−17]

However, there has been no study on the kinetics of SMM migration to the surface. The objective of this work is, therefore, to establish the kinetics of SMM migration by deriving model equations based on experimental data. As a base polymer, PES (poly(ether sulfone)) was chosen since it is one of the most popular materials used to prepare ultrafiltration membranes. SMMs were blended into PES solution, and ultrafiltration membranes were prepared by the phase inversion technique under different conditions. Then, the SMM concentration at the membrane surface was measured.

Experimental Section

Materials. Poly(ether sulfone) (PES, Victrex 4100P) supplied by General Electric was dried at 150 °C for 4 h before use. SMM, the molecular structure of which is given in Figure 2, was synthesized by the method described by Pham et al.[13] in detail. Its weight-average molecular weight determined by the GPC technique was 19 300, and the number-average molecular weight was 13 200 using polystyrene standards. To specify the molecular structure, n and q in Figure 2 are 7 and 2, respectively. m is known to be some value between 4 and 8. In all theoretical calculations m was set equal to 6. *N*-Methylpyrrolidone (NMP) was supplied by Aldrich Chemical Co.

Membrane Preparation. The casting solution containing PES (20 wt %), SMM (1.5 wt %), and NMP (78.5 wt %) were first prepared. A predetermined amount of SMM was added to a 500 mL glass bottle, followed by the addition of NMP. The glass bottle was shaken with an orbital shaker at room temperature for 4 h to fully dissolve the SMM. Then, PES powder was added, and the bottle lid was sealed with a Teflon tape on the riveted neck of the bottle and by an electric tape, or Parafilm, around the outside of the lid and the bottle. To completely mix the polymer, the bottle was placed on the shaker and allowed to shake for at least 24 h. The solution was then filtered through a filter cloth under a pressure of 35−40 psig. The solution was cast on a smooth glass plate to a predetermined thickness using a casting bar. The solvent, NMP, was then evaporated by placing the cast film together with the glass plate in an oven with forced air circulation for a predetermined period. The oven temperature was maintained at 110 °C. The solution film was then immersed in water at 4 °C. Water in membrane was further replaced by ethanol with successive immersion of the membrane in ethanol/water solutions of progressively higher ethanol concentration (overnight for each immersion). Ethanol contents in the solutions were 25, 50, 75, and 100 vol %. Ethanol was subsequently evaporated at room temperature for 24 h to yield final membranes that were subjected to contact angle measurement and XPS analysis. A PES membrane without SMM was also prepared by exactly the same method except for the absence of SMM in the casting solution.

Contact Angle Measurement. The contact angle of the membrane surface was measured using the 14° horizontal beam comparator (22-2000 SERIES). Samples were prepared by cutting the membranes into pieces of 1.5 × 5 cm at random positions. They were placed on the plastic sample plate and fixed with tape. Then, a syringe filled with distilled water was installed to stand vertically. The syringe needle was adjusted 0.5 mm above the membrane surface. Three microliters of water was injected onto the membrane surface, and the position of the moving bed was adjusted so that water drop was fitted to the scale when projected on the screen. The contact angle was measured at four different spots on each membrane sample. Tests were carried out with all membranes prepared.

X-ray Photoelectron Spectroscopy (XPS). The surface of the membranes was analyzed using a Kratos Axis X-ray photoelectron spectrometer (Kratos, Manchester, UK). Samples of 1 mm^2 sizes were taken from random positions of the membrane and analyzed. The analysis method was similar to the angle-resolved XPS technique described by Deslandes et al.[18] for probing thinner layers of the surface. The samples were analyzed at takeoff angles of 0° and 60°, where θ is the angle between the normal to the sample and the detector. At $\theta = 0°$, the sample was perpendicular to the detector, leading to maximum sampling depth. The effective sampling depth, z, according to Deslandes et al.[18] was equal to

$$z = 3\lambda \cos \theta$$

where λ is the effective mean path for electrons to escape the surface. Briggs[19] provided sampling depths for F 1s as a function of takeoff angle. Based on his data, $z = 6.3$ nm at $\theta = 0°$ and 3.15 nm at $\theta = 60°$, which correspond to an effective mean path, λ, of 2.1 nm. According to Clark,[20] λ is 2.3 ± 0.3 nm.

Theoretical Section

A kinetic model for SMM migration that is occurring in the polymer solution film while it is placed in the

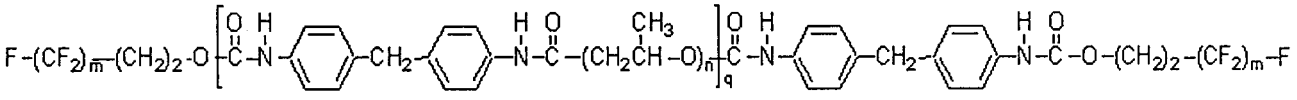

Figure 2. Structure of an SMM.

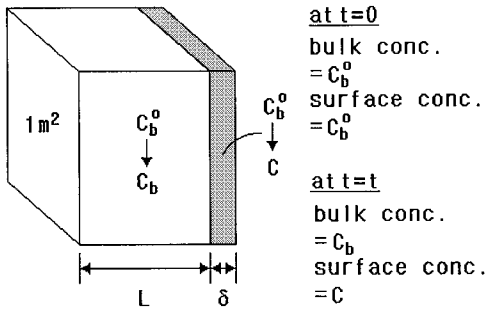

Figure 3. Schematic representation of the bulk and surface layers.

oven was established under the following assumptions. It should be noted that solvent evaporation took place together with the SMM migration.

1. There is a bulk layer of thickness L, out of which SMMs migrate.

2. There is a surface layer of thickness δ, into which SMMs migrate.

3. There is a plane of boundary between the bulk layer and the surface layer through which SMMs migrate.

4. Both L and δ decrease with time as solvent evaporates. However, $L\epsilon$ and $\delta\epsilon$, where ϵ is the volume fraction of polymer (PES + SMM) in the solution, do not change since polymer does not evaporate.

5. Mass transfer through the plane of boundary is accelerated with time because the distance SMM passes through to migrate into the surface layer is shortened as more solvent is evaporated. The mass transfer coefficient is arbitrarily given by

$$k = k^{\circ}t^2 \tag{1}$$

6. The driving force for the SMM migration is (the surface SMM concentration in equilibrium with the bulk SMM concentration − the surface SMM concentration). The migration will stop when the above concentration difference will become zero.

The bulk and surface layer and the SMM concentration in each layer are schematically shown in Figure 3.

Under the above assumptions, the following equations were derived.

$$(c_f^{\infty} - c_f)/(c_f^{\infty} - c_{f,b}^0) = \exp(-\beta t^3) \tag{2}$$

where c_f is the fluorine content at the surface, $c_{f,b}^0$ is c_f at time $t = 0$ and also the fluorine content in the bulk at $t = 0$, and c_f^{∞} is c_f when $t = \infty$ and given by

$$c_f^{\infty} = \{(\alpha(\delta/L) + \alpha)/(\alpha(\delta/L) + 1)\}c_{f,b}^0 \tag{3}$$

α is an equilibrium constant when an linear equilibrium is assumed between the surface and the bulk SMM concentration, and β is a constant given by

$$\beta = k^0(\alpha(\delta/L) + 1)/3\delta\epsilon \tag{4}$$

Results and Discussion

Contact Angle Measurement. Contact angles were measured for a PES membrane and a PES/SMM membrane prepared with zero evaporation time. Three samples were prepared from each membrane, and contact angles at four different spots were measured for each sample. Two out of 12 results were discarded since they were far from the average value. The average contact angles so obtained were both 66°, for PES and PES/SMM membrane. It was therefore concluded that the presence of SMMs did not affect the contact angle, when evaporation time was zero. This indicates that a certain time is necessary for the migration of SMMs toward the membrane surface to occur. PES membranes of a cast thickness 0.12 mm, prepared with three different evaporation periods (3, 5, and 7 min), were then subjected to the contact angle measurement. The average contact angle did not change with a change in evaporation period as shown in Figure 4. This indicates that solvent evaporation has no effect on the contact angle of the PES membranes. Finally, nine PES/SMM membranes of three different cast thickness (0.12, 0.18, and 0.24 mm) with three different evaporation periods (3, 5, and 7 min) were prepared, and the contact angles were measured. The results are also given in Figure 4.

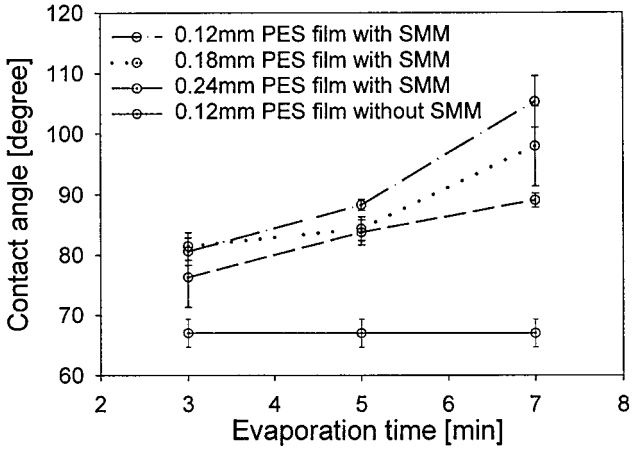

Figure 4. Contact angle vs evaporation time.

The figure shows that the contact angle increased with an increase in evaporation period and also depended on the film thickness. The contact angle tends to be greater as the film thickness becomes smaller. In particular, the contact angle increased from 80° to 106° when the film thickness was 0.12 mm. The increase in contact angle with evaporation time clearly indicates the migration of SMMs toward the surface of the film, while the solvent was being evaporated, rendering the surface more hydrophobic.

XPS Study. Six membranes were prepared with two different thickness (0.12 and 0.24 mm) and three different evaporation periods (3, 5, and 7 min). Two areas were chosen from each membrane and subjected to XPS analysis at two takeoff angles, i.e., 0° and 60°, which correspond to the X-ray sampling depths of 6.3 and 3.15 nm, respectively. All samples contained carbon, oxygen, fluorine, nitrogen, and sulfur, except for some membranes in which no sulfur was detected. It should be noted XPS does not detect hydrogen. The results of XPS analysis are summarized in Tables 1 and 2. In both tables, it is noticed that fluorine contents at the sampling depth of 3.15 nm are higher than those at 6.3 nm. This means that SMMs, which contain fluorine, become more concentrated near the membrane surface. Since the atomic composition of the membrane surface is better represented by the data at the sampling depth of 3.15 nm, those data were chosen in Figure 5 to show the effect of cast film thickness and evaporation period on the atomic percent of fluorine.

It should be noted that the fluorine content at 2000 min of evaporation time was added in Figure 5 to show

Table 1. Atomic Percent[a] Measured by XPS Analysis of SMM Blended Membranes (Cast Film Thickness, 0.12 mm)[b]

	sampling depth					
	3.15 nm			6.3 nm		
evaporation time	3 min	5 min	7 min	3 min	5 min	7 min
carbon (C 1s)	73.0	68.8	57.4	72.8	70.9	63.7
oxygen (O 1s)	16.0	15.8	11.1	16.3	16.8	12.9
fluorine (F 1s)	5.3	9.8	27.8	4.6	6.2	19.2
nitrogen (N 1s)	1.8	2.3	3.7	2.0	2.0	4.2
sulfur (S 2p)	3.8	3.3		4.4	4.1	

[a] Error range is ±5−10%. [b] Theoretical pure PES composition, atomic % without hydrogen: C (75.0), O (18.7), S (6.3). Theoretical pure SMM composition, atomic % without hydrogen: C (64.8), O (15.0), N (3.8), F (16.4).

Table 2. Atomic Percent[a] Measured by XPS Analysis of SMM Blended Membranes (Cast Film Thickness; 0.24 mm)[b]

	sampling depth					
	3.15 nm			6.3 nm		
evaporation time	3 min	5 min	7 min	3 min	5 min	7 min
carbon (C 1s)	71.3	72.4	67.0	72.4	71.3	70.1
oxygen (O 1s)	16.8	16.9	14.4	17.0	17.0	15.9
fluorine (F 1s)	5.9	8.1	13.8	4.3	5.6	8.6
nitrogen (N 1s)	2.0		4.1	1.8	2.7	4.0
sulfur (S 2p)	4.0	2.6	0.8	4.5	2.8	1.4

[a] Error range is ±5−10%. [b] Theoretical pure PES composition, atomic % without hydrogen: C (75.0), O (18.7), S (6.3). Theoretical pure SMM composition, atomic % without hydrogen: C (64.8), O (15.0), N (3.8), F (16.4).

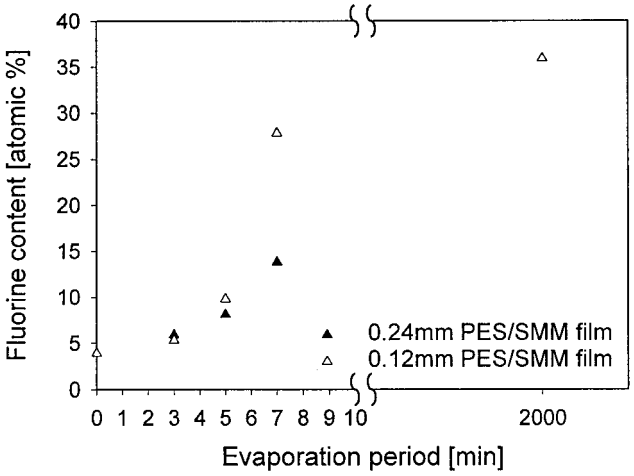

Figure 5. XPS fluorine content vs evaporation time.

that the surface is saturated by SMMs after a long period of solvent evaporation. The figure clearly shows that the fluorine content increases with an increase in evaporation period. It also shows that surface fluorine content is higher when the cast film is thinner. This means that SMMs migrate more to the membrane surface with an increase in evaporation period and decrease in cast film thickness. Hence, the results from XPS experiments agree with those from contact angle measurements.

Experimental Verification of the Kinetic Model. The experimental data for a cast film thickness of 0.12 mm and a X-ray sampling depth of 3.15 nm were simulated by eq 2 by setting $c_{f,b}^0$ and c_f^∞ equal to 3.9 and 35.9 atomic % fluorine, respectively, which were the experimental values. The parameter β was obtained by linear regression analysis. The line in Figure 6 indicates

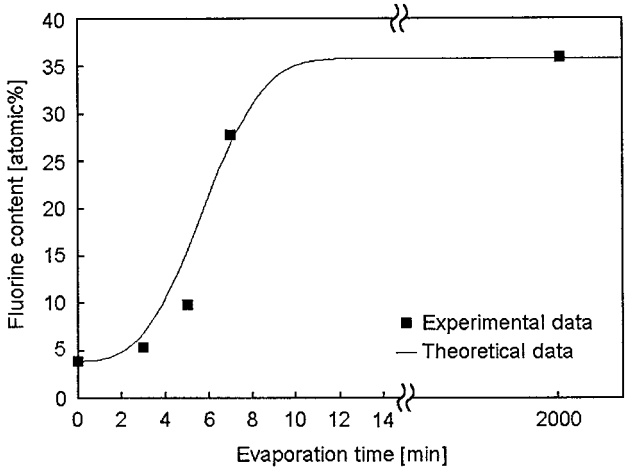

Figure 6. Comparison of experimental XPS values with the results from theoretical calculations.

the theoretical values calculated by eq 2. The experimental fluorine contents were plotted along with the experimental line. The simulation represents the experimental values satisfactorily. In particular, the initial lag time and the tendency for fluorine content to level off at the final stage of evaporation period are well represented by the theoretical line.

Despite satisfactory agreement between the model calculation and the experiment, it should be admitted that the model seems to be oversimplification. In particular, it is a serious drawback that the model cannot predict any SMM concentration profile in the X-ray depth direction that was observed experimentally. It should be also pointed out that the fluorine content obtained by XPS experiments does not necessarily agree with the fluorine content calculated on the basis of SMM/PES molar ratio. For example, the fluorine content that corresponds to the initial weight ratio of SMM/PES = 7/93 should be equal to 1.14 atomic %, while the initial bulk fluorine content is 3.9 atomic %. The maximum fluorine content achieved was 35.9 atomic %, as stated earlier, which is far greater than the theoretical fluorine content of 16 atomic % for pure SMM. The ratio of the final surface concentration to the initial bulk concentration is 16/0.85 = 18.8 according to the theory while it is 35.9/3.9 = 9.2 by experiment.

The experimental fluorine contents higher than the theoretical values suggest the preferential orientation of fluorine end group at the outermost surface of the membrane.

Assuming $m = 6$ and also assuming that the fluorocarbon end groups ($-C_6F_{13}$) of SMMs cover the surface, the thickness of the fluorocarbon overlayer, d, is calculated by the following equation.[21]

$$d = (\lambda/\cos\theta)\ln[1 + c_{fc}/(1 - c_{fc})] \qquad (5)$$

where c_{fc} is the concentration of fluorine and carbon atoms (%) that are present in fluorocarbon end groups.

Using the data given in Tables 1 and 2 for the fluorine atomic percent at the lower sampling depth (3.15 nm) and the longest evaporation time (7 min), c_{fc} can be calculated as follows. In Table 1, fluorine atomic % is 27.8. Since there are six carbon atoms and 13 fluorine atoms in a fluorocarbon end group, c_{fc} is $(1 + 6/13) \times 27.8 = 40.6\%$. Similarly, from Table 2 c_{fc} is calculated to be 20.2%. Then, d becomes

$d = (2.5/\cos 60°) \ln[1 + 0.406/(1 - 0.406)] = 2.60$ nm

and

$d = (2.5/\cos 60°) \ln[1 + 0.202/(1 - 0.202)] = 1.13$ nm

Using bond lengths of 0.158 and 0.138 nm for C−C and C−F, respectively, and a bond angle of 109.5° for C−C−C, the length for the fluorocarbon chain with $m = 6$ is calculated to be 0.75 nm. This value is smaller than, however, is comparable to the overlayer thickness calculated above.

Conclusions

The following conclusions were drawn from the experimental data and the results of the theoretical calculations.

1. SMMs migrate to the surface during solvent evaporation from the cast films as evidenced by contact angle measurement and XPS.
2. The SMMs are preferentially oriented with fluorocarbon end groups at the outermost surface of the membrane.
3. A model proposed for the kinetics of SMM surface migration can represent the data from XPS experiments satisfactorily.
4. About 10 min is required to complete the SMM surface migration under the experimental conditions adopted in this work.

Acknowledgment. Authors gratefully acknowledge the financial support of Materials and Manufacturing Ontario.

References and Notes

(1) Strathmann, H. In *Handbook of Industrial Membrane Technology*; Porter, M. C., Ed.; Noyes Publications: Park Ridge, NJ, 1990.
(2) Mulder, M. In *Basic Principles of Membrane Technology*; Kulwer Academic: Norwell, MA, 1996.
(3) Cadotte, J. E. US Patent US4277344, 1981.
(4) Ganbassi, F.; Morra, M.; Occhiello, E. In *Polymer Surfaces from Physics to Technology*; John Wiley & Sons: New York, 1996.
(5) Matsuura, T.; Santerre, P.; Narbaitz, R. M.; Fang, Y.; Pham, V. A.; Mahmud, H.; Baig, F. US Patent US5954966, 1999.
(6) Pan, D. H.-K.; Prest, Jr., W. M. *J. Appl. Phys.* **1985**, *58*, 2861−2870.
(7) Bhatia, Q. S.; Pan, D. H.; Koberstein, J. T. *Macromolecules* **1988**, *21*, 2166−2175.
(8) Thomas, H. R.; O'Malley, J. J. *Macromolecules* **1979**, *12*, 323−329.
(9) O'Malley, J. J.; Thomas, H. R.; Lee, G. M. *Macromolecules* **1979**, *12*, 996−1001.
(10) Schmidt, J. J.; Gardella, Jr., J. A.; Salvati, Jr., L. *Macromolecules* **1989**, *22*, 4489−4495.
(11) Hamza, A. V.; Pham, V. A.; Matsuura, T.; Santerre, J. P. *J. Membr. Sci.* **1997**, *131*, 217−227.
(12) Suk, D. In *Comprehensive Exam Report*; Department of Chemical Engineering, University of Ottawa: Ottawa, Canada, 2000.
(13) Pham, V. A.; Santerre, J. P.; Matsuura, T.; Narbaitz, R. M. *J. Appl. Polym. Sci.* **1999**, *73*, 1363−1378.
(14) Mahmud, H. M.A.Sc. Thesis, Department of Chemical Engineering, University of Ottawa, Ottawa, Canada, 1996.
(15) Ho, J. Y.; Matsuura, T.; Santerre, J. P. *J. Biomater. Sci., Polym. Ed.* **2000**, *11*, 1085−1104.
(16) Fang, Y.; Pham, V.; Matsuura, T.; Santerre, J. P.; Narbaitz, R. M. *J. Appl. Polym. Sci.* **1994**, *54*, 1937−1943.
(17) Minnery, J. G. M.A.Sc. Thesis, Department of Chemical Engineering, University of Ottawa, Ottawa, Canada, 2000.
(18) Deslandes, Y.; Pleizer, G.; Alexander, D.; Santerre, P. *Polymer* **1998**, *39*, 2361−2366.
(19) Briggs, D. In *Surface Analysis of Polymers by XPS and Static SIMS*; Cambridge University Press: Cambridge, U.K., 1998.
(20) Clark, D. T.; Thomas, H. R. *J. Polym. Sci., Polym. Chem. Ed.* **1977**, *15*, 2843.
(21) Ertl, G.; Kuppers, J. In *Low Energy Electrons and Surface Chemistry*; VCH: Deerfield Beach, FL, 1985.

MA011205A